Journal of Cerebral Blood Flow & Metabolism (2011) 31, 881–893

www.jcbfm.com

Vascular adhesion protein-1 inhibition provides antiinflammatory protection after an intracerebral hemorrhagic stroke in mice

Qingyi Ma[1], Anatol Manaenko[1], Nikan H Khatibi[2], Wanqiu Chen[1], John H Zhang[1,2,3] and Jiping Tang[1]

[1]*Department of Physiology and Pharmacology, Loma Linda University, Loma Linda, California, USA;* [2]*Department of Anesthesiology, Loma Linda Medical Center, Loma Linda, California, USA;* [3]*Department of Neurosurgery, Loma Linda Medical Center, Loma Linda, California, USA*

The systemic immune response has a vital role in propagating the damage of an intracerebral hemorrhage (ICH). Vascular adhesion protein-1 (VAP-1), a semicarbazide (SCZ)-sensitive-amine-oxidase, was found in previous studies to have a role in migration of immune cells. In this study, we hypothesize that VAP-1 inhibition may decrease brain injury by attenuating the transmigration of immune cells to the injury site, and by doing so, reduce cerebral edema and improve neurobehavioral function in mice. Two VAP-1 inhibitors, LJP1586 and SCZ were given 1 hour after ICH induction by either collagenase or autologous blood injection. The VAP-1 siRNA, a VAP-1 gene silencer, and human recombinant AOC3 protein, a VAP-1 analogue, were delivered by intracerebroventricular injection. Postassessment included neurobehavioral testing, brain edema measurement, quantification of neutrophil infiltration and microglia/macrophage activation, and measurement of intercellular adhesion molecule-1 (ICAM-1), P-selectin, monocyte chemoattractant protein-1 (MCP-1), and tumor necrosis factor-α (TNF-α) expression 24 hours after ICH. We found that LJP1586 and SCZ reduced brain edema and neurobehavioral deficits 24 hours after ICH induction. These two drugs were also found to decrease levels of ICAM-1, MCP-1, TNF-α, and inhibit neutrophilic infiltration and microglia/macrophage activation. We conclude that VAP-1 inhibition provided antiinflammation effect by reducing adhesion molecule expression and immune cell infiltration after ICH.
Journal of Cerebral Blood Flow & Metabolism (2011) **31,** 881–893; doi:10.1038/jcbfm.2010.167; published online 29 September 2010

Keywords: antiinflammation; brain edema; inflammation; intracerebral hemorrhage; vascular adhesion protein-1

Introduction

Intracerebral hemorrhage (ICH) is a fatal stroke subtype that affects roughly 120,000 individuals in the United States each year (Ribo and Grotta, 2006). Responsible for 10% to 15% of all strokes, ICH accounts for one of the highest morbidity and mortality rates, leaving those individuals who survive with lasting disabilities (Dennis *et al*, 1993). As the population in the world continues to shift toward an aged majority, the incidence of ICH will be expected to grow, and the demand for a better understanding of the pathophysiology will be expected.

The inflammatory response in an ICH is characterized by activation of local immune cells such as microglial cells. This local inflammatory reaction is partly responsible for the damages to the brain after injury. However, mounting evidence suggests that accumulation of systemic immune cells, specifically blood-derived leukocytes, are the primary orchestrators of this damage (Wang and Dore, 2007). Infiltration of these systemic immune cells result in enhanced disruption of the blood–brain barrier causing an increase in cerebral edema formation, and subsequent deterioration in neurobehavioral function. As a result, studies have redirected their attention to focus more on preventative measures that can decrease the accumulation of systemic immune cells to the site of injury. In focal ischemic stroke models, investigators found that systemic immune cell recruitment was mediated in part by the increase in adhesion molecule expression along

Correspondence: Dr J Tang, Department of Physiology and Pharmacology, Loma Linda University School of Medicine, Loma Linda, CA 92354, USA.
E-mail: jtang@llu.edu
This study was partially supported by NIH NS060936 to JPT and NS053407 to JHZ.
Received 9 April 2010; revised 10 August 2010; accepted 27 August 2010; published online 29 September 2010

the endothelial cell walls (Yilmaz and Granger, 2008). As a result, these systemic immune cells propagated the local immune response by releasing proinflammatory cytokines at the site of injury, increasing cerebral edema and worsening neurobehavioral function (Aronowski and Hall, 2005; Barone and Feuerstein, 1999; Emsley and Tyrrell, 2002).

Vascular adhesion protein-1 (VAP-1), a cell-surface expressed glycoprotein, has recently emerged as a potential target for inflammatory regulation in the brain. Classified as a semicarbazide (SCZ)-sensitive-amine-oxidase (Salmi and Jalkanen, 1992), VAP-1 can also function as an adhesion molecule, promoting leukocyte adhesion and transmigration. Under normal conditions, VAP-1 is expressed within cytosolic vesicles of endothelial cells where it remains dormant. However, under inflammatory conditions, VAP-1 migrates to the luminal surface of endothelial cells within the blood vessels, where it mediates binding and transmigration of systemic immune cells into tissues, disrupting the blood–brain barrier along with it (Salmi and Jalkanen, 2005).

As a result in this study, we investigated the role of VAP-1 in ICH-induced brain injury, specifically investigating its role in regulating the systemic immune response. We hypothesize that VAP-1 blockage will attenuate the infiltration of systemic immune cells by downregulating adhesion molecule expression and therefore, improve neurologic outcomes. To test this aim, we used a small molecule VAP-1 inhibitor, LJP1586 (O'Rourke *et al*, 2008) to inhibit the VAP-1 activity. In addition, as the SCZ-sensitive-amine-oxidase enzyme activity is necessary for leukocyte transmigration (Koskinen *et al*, 2004), another VAP-1 inhibitor, SCZ, was used as testament to the antiinflammatory effects of LJP1586. In addition, we injected VAP-1 siRNA, a VAP-1 gene silencer, to specify the inhibition of VAP-1, as well as recombinant AOC3 protein, a VAP-1 analogue, to neutralize the effect of LJP1586.

Materials and methods

Animals

All procedures for this study were approved by the Animal Care and Use Committee at Loma Linda University and complied with the NIH Guide for the Care and Use of Laboratory Animals (National Institutes of Health Publication 85-23, revised 1985) and with the Guidelines for the Use of Animals in Neuroscience Research by the Society for Neuroscience. Eight-week-old male CD1 mice (weight 35 to 45 g; Charles River, Wilmington, MA, USA) were housed in a 12-hour light/dark cycle at a controlled temperature and humidity with free access to food and water. During surgery, body temperature was monitored and kept constant. Following surgery using one of the two established models, either the collagenase-ICH (cICH), or blood-ICH (bICH), the skull hole was closed with bone wax, the incision was closed with sutures, and the mice were allowed to recover. To avoid postsurgical dehydration, 0.5 mL of normal saline was given to each mouse by subcutaneous injection immediately after surgery.

Intracerebral Hemorrhage Mouse Models and Treatment

Intracerebral hemorrhage model was induced by collagenase injection (cICH) as previously described (Rosenberg *et al*, 1990; Tang *et al*, 2004, 2005) (Figure 1). Briefly, mice were anesthetized with ketamine (100 mg/kg) and xylazine (10 mg/kg) (2:1 v/v, intraperitoneal injection) and positioned prone in a stereotactic head frame (Kopf Instruments, Tujunga, CA, USA). A cranial burr hole (1 mm) was drilled near the right coronal suture 1.4 mm lateral to the midline. A 27-gauge needle was inserted stereotactically into the right basal ganglia coordinates: 0.9 mm posterior to the bregma, 1.4 mm lateral to the midline, and 4 mm below the dura. Collagenase (VII-S, Sigma, St Louis, MO, USA; 0.075 U in 0.5 μL of saline) was infused into the brain over 2 minutes at a rate of 0.25 μL/min with a microinfusion pump (Harvard Apparatus, Holliston, MA, USA). Sham-operated mice were subjected to needle insertion only. The needle was left in place for an additional 10 minutes after injection to prevent possible leakage of the collagenase solution.

Three experiments were performed in the cICH model. (1) Mice were divided into four groups: sham ($n = 22$), vehicle (ICH, $n = 32$), LJP1586 treatment (3 and 10 mg/kg, intraperitoneal injection, $n = 37$), and SCZ treatment (100 and 200 mg/kg, intraperitoneal injection, $n = 30$). Both drugs were dissolved in phosphate-buffered saline (PBS; pH 7.4) and given 1 hour after ICH induction. Both sham and vehicle animals received the same volume of PBS injection. (2) The VAP-1 siRNA (Sigma Aldrich) was dissolved in sterilized water and given (100 pmol, 2 μL, intracerebroventricular injection) 48 hours before ICH. The same volume of scramble siRNA (siGENOME nontargeting siRNA; Thermol Fisher Scientific, Pittsburgh, PA, USA) was administered as control. The animals were divided into five groups, sham ($n = 8$), vehicle (ICH, $n = 8$), siRNA plus sham ($n = 12$), siRNA plus ICH ($n = 12$), and scramble siRNA plus ICH groups ($n = 12$). (3) Human recombinant AOC3 (VAP-1) protein (Abnova Co, Walnut, CA, USA) was given 10 minutes before ICH induction to neutralize the effects of LJP1586. Mice were divided into five groups: sham ($n = 8$), vehicle (ICH, $n = 6$), AOC3 (30 ng, 90 ng/animal, intracerebroventricular injection) plus LJP1586 (10 mg/kg, intraperitoneal injection, $n = 22$), AOC3 plus sham ($n = 6$), and AOC3 plus ICH group ($n = 10$).

The ICH was induced using the autologous blood injection model (bICH), which was modified from previous descriptions (Belayev *et al*, 2003; Rynkowski *et al*, 2008; Wang *et al*, 2008). Briefly, mice were anesthetized with ketamine (100 mg/kg) and xylazine (10 mg/kg) (2:1 v/v, intraperitoneal injection) and positioned prone in a stereotactic head frame (Kopf Instruments). A scalp incision was made along the midline and a burr hole (1 mm) was drilled on the right side of the skull (0.2 mm anterior and 2.0 mm lateral of the bregma). The mouse tail was warmed with hot water for 2 minutes and then cleaned

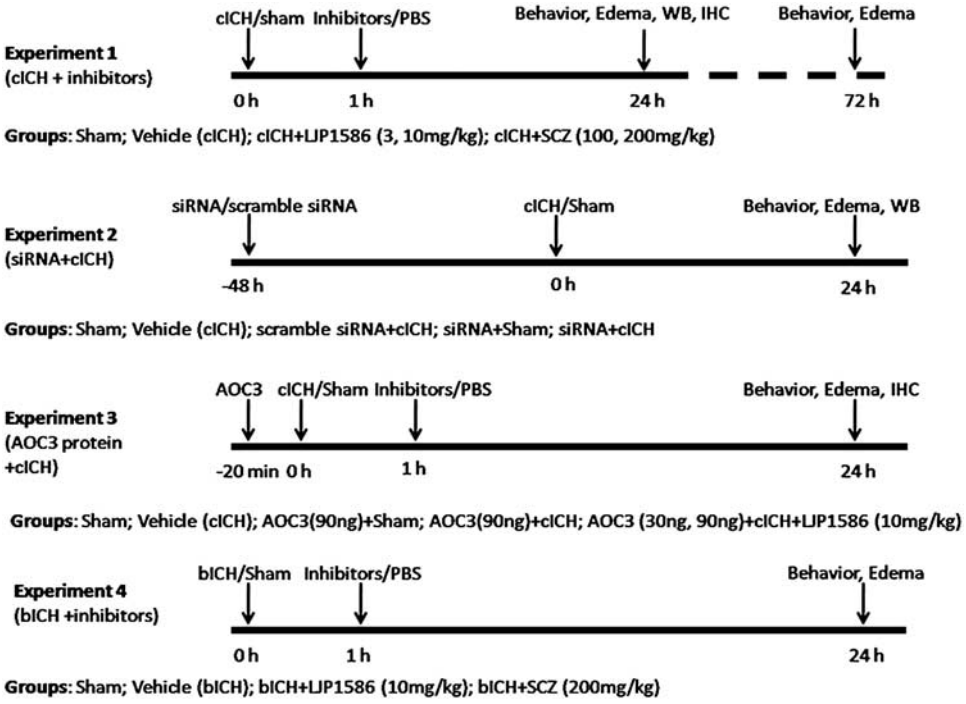

Figure 1 Experimental design and animal group classification.

with 70% ethanol before cutting off 10 mm of the tail tip with sterilized surgical scissors. Next, 30 μL of autologous tail blood was collected in a capillary tube without heparin and blown into a 1-mL insulin syringe. The syringe was fixed onto the microinjection pump, whereas the needle was stereotaxically inserted into the brain through the burr hole. At first, the needle was stopped at 0.7 mm above the target position and 5 μL of blood was delivered at a rate 2 μL/min. The needle was then advanced to the target position. After 7 minutes, the remaining 25 μL blood was injected at a rate of 2 μL/min. The needle was left in place for an additional 10 minutes after injection to prevent possible leakage and withdrawn slowly in 7 minutes.

Mice were treated with LJP1586 (10 mg/kg, intraperitoneal injection, $n=6$) or SCZ (200 mg/kg, intraperitoneal injection, $n=6$) 1 hour after ICH induction. We also did sham ($n=6$) and vehicle group ($n=7$).

All animals were neurologically tested and killed 24 or 72 hours after ICH induction. Evaluation of neurologic function was performed by a masked investigator. Brain samples were collected for measurement of brain water content, Western blot or immunohistochemistry.

Vascular Adhesion Protein-1 siRNA Injection

siRNA was administered by intracerebroventricular injection to the mouse brain as previously described (Luo *et al*, 2007). Briefly, mice were anesthetized with ketamine (100 mg/kg) and xylazine (10 mg/kg) (2:1 v/v, intraperitoneal injection) and positioned prone in a stereotactic head frame (Kopf Instruments). A scalp incision was made along the midline and a burr hole (1 mm) was drilled in the right side of the skull (1.0 mm lateral of the bregma). According to the manufacture's instructions, 2 μL (100 pmol) of VAP-1 siRNA (Sigma) suspended in sterile water or scramble siRNA was delivered into the ipsilateral ventricle with a Hamilton syringe over 2 minutes. The needle was left in place for an additional 5 minutes after injection to prevent possible leakage and then withdrawn slowly in 4 minutes. After the removal of the needle, the burr hole was sealed with bone wax, the incision was closed with sutures and the mice were allowed to recover. Intracerebral hemorrhage induced by collagenase injection was conducted 48 hours later. Mice were killed for edema measurement and VAP-1 protein expression 24 hours after ICH. We did not measure the ICP because of the size challenges that mice impose. Furthermore, multiple invasive operations can affect study results quite unfavorably.

Human Recombinant AOC3 (Vascular Adhesion Protein-1) Protein Injection

Human recombinant AOC3 (VAP-1) protein (Abnova Co.) was administered in the same manner as the VAP-1 siRNA injection described above. According to the manufacture's instruction, 1 μL (30 ng/mouse) or 3 μL (90 ng/mouse) protein solutions was delivered into the ipsilateral ventricle with a Hamilton syringe at a rate of 0.5 μL/min. The needle was left in place for an additional 5 minutes after injection to prevent possible leakage and withdrawn slowly in 4 minutes. After the removal of the needle, the burr hole was sealed with bone wax. The collagenase was then injected into the ipsilateral basal ganglia to induce hemorrhage. Afterwards, the incision was closed with sutures, and the mice were allowed to recover. Mice were killed for edema measurement 24 hours after ICH induction.

Hemorrhage Volume

Hemoglobin assay was used as previously described (Tang *et al*, 2005). Briefly, mice were killed 24 hours after ICH and transcardially perfused with ice PBS. Both ipsilateral and contralateral hemisphere were collected and kept in a −70°C freezer. The ipsilateral hemisphere was homogenized for 60 seconds in a tube with distilled water (total volume 3 mL). After centrifugation (12,000 *g*, 30 minutes), 400 μL Drabkin's reagent (Sigma-Aldrich) was added into a 100-μL aliquots of the supernatant and allowed to react for 15 minutes. The absorbance of this solution was read with a spectrophotometer (540 nm), and the amount of blood in each brain was calculated using a standard curve generated with known blood volumes.

Neurobehavioral Function Test

Neurobehavioral functions were evaluated by the modified Garcia test (Garcia *et al*, 1995; Wu *et al*, 2010). In the modified Garcia test, four items including side stroke, vibrissae touch, limb symmetry, and lateral turning were tested with a maximum neurologic score able to be achieved at 12 (healthy animal). We also performed the beam balance test (Zausinger *et al*, 2000) and modified wire-hanging test (Gerlai *et al*, 2000) to further assess neurobehavior. The maximum score able to be reached per test was 5 (data not shown). The behavior test was conducted at different time point after ICH induction by a masked investigator.

Brain Water Content Measurement

Brain water content was measured as previously described (Tang *et al*, 2004, 2005; Tejima *et al*, 2007). Briefly, mice were decapitated under deep anesthesia. Brains were immediately removed and cut into 4 mm sections. Each section was divided into four parts: ipsilateral and contralateral basal ganglia, and ipsilateral and contralateral cortex. The cerebellum was collected as an internal control. Tissue samples were weighed on an electronic analytical balance (APX-60, Denver Instrument, Bohemia, NY, USA) to the nearest 0.1 mg to obtain the wet weight (WW). The tissue was then dried at 100°C for 24 hours to determine the dry weight (DW). Brain water content (%) was calculated as $[(WW-DW)/WW] \times 100$.

Western Blotting

Western Blotting was performed as described previously (Chen *et al*, 2008; Ostrowski *et al*, 2005). Animals were euthanized 24 hours after ICH. Intracardiac perfusion with cold PBS (pH 7.4) solution was performed, followed by removal of the brain and separation into ipsilateral and contralateral cerebrums. The brain parts were stored appropriately at −80°C immediately until analysis. Protein extraction from whole-cell lysates were obtained by gently homogenizing them in RIPA lysis buffer (Santa Cruz Biotechnology, Inc, Santa Cruz, CA, USA, sc-24948) with further centrifugation at 14,000 *g* at 4°C for 30 minutes. The supernatant was used as whole-cell protein extract, and the protein concentration was determined using a detergent compatible assay (Bio-Rad, Hercules, CA, USA, Dc protein assay). Equal amounts of protein (50 μg) were loaded on an SDS-PAGE gel. After being electrophoresed and transferred to a nitrocellulose membrane, the membrane was blocked and incubated with the primary antibody overnight at 4°C. The primary antibodies were goat polycolonal anti-intercellular adhesion molecule (anti-ICAM-1) (Santa Cruz Biotechnology, 1:500), goat polyclonal anti-P-selectin (Santa Cruz Biotechnology, 1:500), rabbit polyclonal anti-monocyte chemoattractant protein-1 (anti-MCP-1) (Abcam, Cambridge, MA, USA, 1:1000), and rabbit polyclonal anti-tumor necrosis factor-α (anti-TNF-α) (Millipore, Temecula, CA, USA, 1:1000). Nitrocellulose membranes were incubated with secondary antibodies (Santa Cruz Biotechnology) for 1 hour at room temperature. Immunoblots were then probed with an ECL Plus chemiluminescence reagent kit (Amersham Biosciences, Arlington Heights, IL, USA) and visualized with the imagine system (Bio-Rad, Versa Doc, model 4000). The data were analyzed by the software Image J.

Assessment of Histology

At 24 hours after ICH, mice were perfused under deep anesthesia with cold PBS (pH 7.4), followed by infusion of 4% paraformaldehyde. The brains were then removed and fixed in formalin at 4°C for a minimum of 3 days. The brains were then dehydrated with 30% sucrose in PBS (pH 7.4) and the frozen coronal slices (10 μm thick) were then sectioned in cryostat (CM3050S; Leica Microsystems, Bannockburn, IL, USA). Immunohistochemistry was performed (Titova *et al*, 2008) using the following primary antibodies: rabbit anti-Iba-1 antibody (Wako Chemicals USA, Inc, Richmond, VA, USA) and rabbit anti-human myeloperoxidase polyclonal antibody (1:300; Dako Cytomation Inc., Carpinteria, CA, USA). The positive cell numbers were counted as previously described (Wang and Dore, 2008). The number of immunoreactive cells from 12 locations per mouse (three sections per mouse, four fields per section, $n=4$, microscopic field $\times 20$) were averaged and expressed as positive cells per field.

Statistical Analysis

Data were expressed as means ± s.e.m. Statistical difference between the two groups was analyzed using the *t*-test. Multiple comparisons were statistically analyzed with one-way analysis of variance followed by Tukey multiple comparison *post hoc* analysis or Student–Newman–Keuls test. A P value of <0.05 was considered statistically significant. For the rating scale data (neurobehavioral test), data were expressed as median ± 25th to 75th percentiles. We used the Kruskal–Wallis one-way analysis of variance on ranks, followed by the Steel–Dwass multiple comparisons tests. For the Western blot data, we used the Kruskal–Wallis one-way analysis of variance on ranks, followed by the Student–Newman–Keuls method for pairwise multiple comparison procedures.

Results

Vascular Adhesion Protein-1 Inhibition Has No Effect on Hemorrhagic Volume

Hemorrhagic volume was estimated at 24 hours after collagenase injection by hemoglobin assay with spectrophotometry (Tang *et al*, 2005). There was no statistical difference observed between cICH vehicle mice and 10 mg/kg LJP1586-treated mice ($38.712 \pm 2.35\,\mu$L, $n=8$ and $39.03 \pm 2.32\,\mu$L, $n=8$, respectively; $t_{14} = -0.0969$, $P = 0.924$; Figure 2A).

Neurobehavioral Deficits Improve with Vascular Adhesion Protein-1 Inhibitors

Two VAP-1 inhibitors were applied after cICH. LJP1586 is a selective, novel small molecule inhibitor of rodent and human VAP-1 activity with relative little effects on other monoamine oxidases. Its antiinflammation effects have been studied in LPS-induced lung inflammation (O'Rourke *et al*, 2008). Semicarbazide, a reference compound for inhibiting SCZ-sensitive-amine-oxidase activity, was the other VAP-1 inhibitor (Mercier *et al*, 2007).

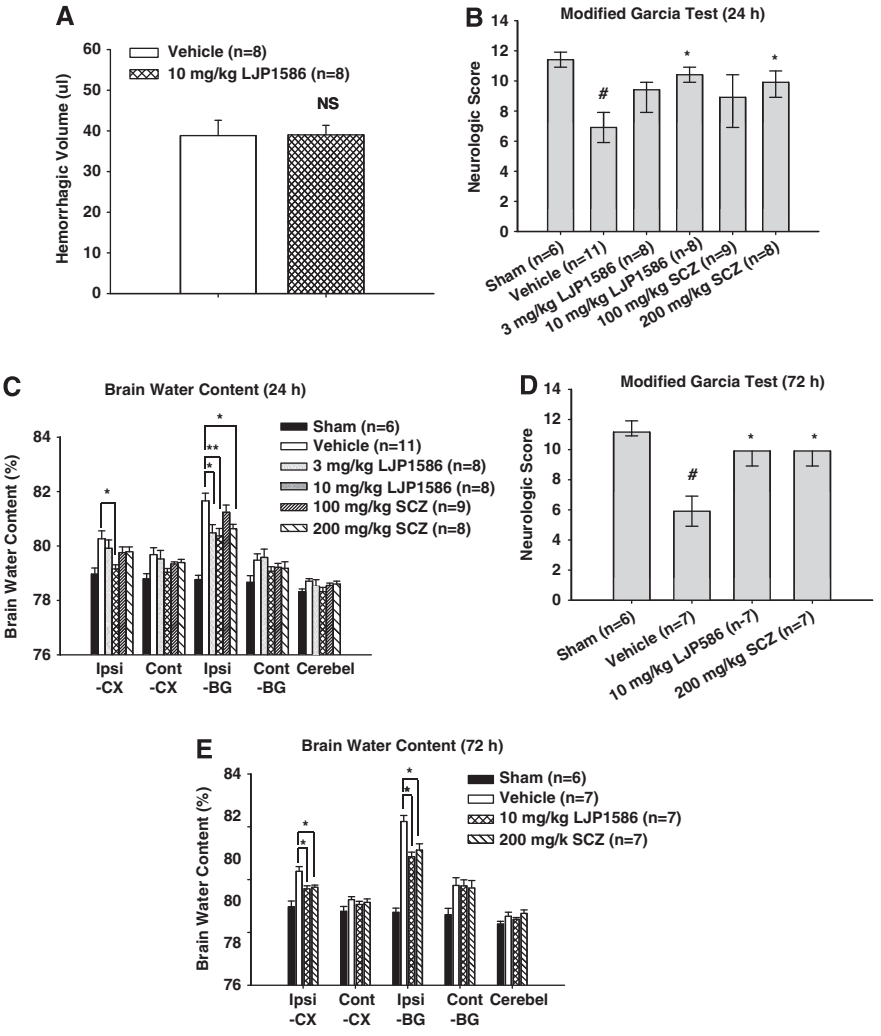

Figure 2 Effect of vascular adhesion protein-1 (VAP-1) inhibitors, LJP1586 and semicarbazide (SCZ) on hemorrhagic volume, neurologic score, and brain water content at 24 and 72 hours after collagenase-intracerebral hemorrhage (cICH) in mice. (**A**) Result of hemoglobin assay for hemorrhagic volume in vehicle ($n = 8$) and LJP1586 (10 mg/kg)-treated mice ($n = 8$). NS, nonsignificant. (**B**) The neurologic score for the modified Garcia test (healthy animal: 12) at 24 hours in sham, ICH, and ICH with treatments (LJP1586: 3 and 10 mg/kg; SCZ: 100 and 200 mg/kg). (**C**) VAP-1 inhibitors, LJP1586 and SCZ reduced brain water content at 24 hours after cICH in mice. Brain samples were collected from sham, ICH, and ICH with treatments (LJP1586: 3 and 10 mg/kg; SCZ: 100 and 200 mg/kg). (**D**) The neurologic score for the modified Garcia test (healthy animal: 12) at 72 hours in sham, ICH, and ICH with treatments (LJP1586:10 mg/kg; SCZ: 200 mg/kg). (**E**) VAP-1 inhibitors, LJP1586 and SCZ reduced brain water content at 72 hours after cICH in mice. Brain samples were collected from sham, ICH, and ICH with treatments (LJP1586: 10 mg/kg; SCZ: 200 mg/kg). Brain sections (4 mm) were divided into four parts: ipsilateral basal ganglia (Ipsi-BG), ipsilateral cortex (Ipsi-CX), contralateral basal ganglia (Cont-BG), and contralateral cortex (Cont-CX). Cerebellum (Cerebel) is the internal control. $^{\#}P < 0.05$ versus sham group. $^{*}P < 0.05$ versus vehicle group. $^{**}P < 0.01$ versus vehicle group.

To evaluate the sensorimotor deficits after cICH, the modified Garcia test was conducted at both 24 and 72 hours post-cICH. The results showed that vehicle mice presented with severe neurobehavioral deficits compared with sham mice ($P<0.05$ versus sham). However, after treatment with high-dose LJP1586 (10 mg/kg) and high-dose SCZ (10 mg/kg), a significant improvement in neurobehavioral function was seen with the modified Garcia test at both 24 and 72 hours ($P<0.05$ versus vehicle, Figures 2B and 2D). For the beam balance test, a significant improvement in neurobehavioral function was seen after treatment with high-dose LJP1586 and high-dose SCZ at both 24 and 72 hours ($P<0.05$ versus vehicle, data not shown); however, in the wire-hanging test, high-dose LJP1586 (10 mg/kg) dramatically improved neurobehavioral function compared with vehicle group at both 24 and 72 hours ($P<0.05$ versus vehicle, data not shown), whereas high-dose SCZ significantly improved neurobehavioral function only at 72 hours ($P<0.05$ versus vehicle, data not shown).

Overall, it was found that VAP-1 inhibitors could improve neurobehavioral functions in a cICH model at both acute and delayed stages.

Brain water content was also measured 24 and 72 hours post-cICH (Figures 2C and 2E). After treatment with low-dose (3 mg/kg) and high-dose (10 mg/kg) LJP1586, brain edema was found to be significantly reduced in the ipsilateral basal ganglia compared with vehicle groups (ipsilateral basal ganglia: 24 hours, 3 mg/kg, 80.53 ± 0.30 versus vehicle, 81.82 ± 0.32, $P<0.05$; 10 mg/kg, 80.41 ± 0.27 versus vehicle, 81.82 ± 0.32, $P<0.01$; 72 hours, 10 mg/kg, 80.92 ± 0.17 versus vehicle, 82.96 ± 0.21, $P<0.05$). In the ipsilateral cortex, high-dose LJP1586 (10 mg/kg) significantly reduced brain edema compared with vehicle (ipsilateral cortex: 24 hours, 10 mg/kg, 79.21 ± 0.15 versus vehicle, 80.31 ± 0.29, $P<0.05$; 72 hours, 79.70 ± 0.12 versus vehicle, 80.37 ± 0.18, $P<0.05$). With high-dose SCZ treatment (200 mg/kg), brain edema decreased in the ipsilateral basal ganglia compared with vehicle at both 24 and 72 hours (ipsilateral basal ganglia: 24 hours, 200 mg/kg, 80.68 ± 0.16 versus vehicle, 81.82 ± 0.32, $P<0.05$; 72 hours, 81.17 ± 0.24 versus vehicle, 82.96 ± 0.21, $P<0.05$); however, in the ipsilateral cortex, only posttreatment at 72 hours significantly reduced brain water content (ipsilateral cortex: 200 mg/kg, 79.76 ± 0.10 versus vehicle, 80.37 ± 0.18, $P<0.05$).

Vascular Adhesion Protein-1 Inhibitors Downregulate Levels of Intercellular Adhesion Molecule-1, Monocyte Chemoattractant Protein-1 (MCP-1), and Tumor Necrosis Factor-α After Intracerebral Hemorrhage Injury

In an *in vitro* study, VAP-1 was found to produce biologically active mediators that could act as signals to induce expression of E- and P-selectins, as well as ICAM-1 in endothelial cells (Jalkanen *et al*, 2007). As a result, we investigated whether VAP-1 activity had any effect on the expression of adhesion molecules, that is ICAM-1, P-selectin, 24 hours post-ICH injury. In addition, in the development of choroidal neovascularization, the expression of a number of inflammatory molecules such as TNF-α and MCP-1 was suppressed after VAP-1 blockade (Noda *et al*, 2008). As a result, we also studied the effect of VAP-1 inhibition on cytokine expression, looking specifically at MCP-1 and TNF-α.

Our results demonstrated that cICH injury produced a significant increase in the expression of P-selectin ($P<0.05$ versus sham, Figure 3A) and ICAM-1 ($P<0.01$ versus sham, Figure 3B). Treatment with high-dose LJP1586 (10 mg/kg) and SCZ (200 mg/kg) significantly decreased the expression of P-selectin ($P<0.05$ versus sham, Figure 3A) and ICAM-1 ($P<0.05$ versus vehicle, Figure 3B). Levels of the proinflammatory cytokines MCP-1 and TNF-α were significantly increased 24 hours post-cICH (MCP-1, $P<0.01$; TNF-α, $P<0.05$ versus sham, Figures 3C and 3D). Treatment with high-dose LJP1586 (10 mg/kg) and SCZ (200 mg/kg) markedly reduced the level of MCP-1 and TNF-α ($P<0.05$ versus vehicle, Figures 3C and 3D).

Vascular Adhesion Protein-1 Inhibition Blocks Migration of Systemic Neutrophils and Microglia/Macrophage Activation

To determine the effect VAP-1 had on inflammatory cells, we checked neutrophilic infiltration by MPO staining and microglia/macrophage activation by Iba-1 staining. At the same time, quantification of both the MPO and Iba-1-positive cells in the perihematomal area were determined. The results demonstrated that posttreatment with LJP1586 at 24 hours showed a significant reduction in the MPO-positive cell numbers (11.89 ± 2.57, $n=4$ and 25.03 ± 1.31, $n=4$, respectively; $t_6=4.547$, $P=0.01$; Figures 4A and 4C), whereas the microglia/macrophage activation was also attenuated in the perihematomal area compared with vehicle mice (4.23 ± 0.57, $n=4$ and 7.81 ± 0.50, $n=4$, respectively; $t_6=4.731$, $P=0.003$; Figures 4D and 4E).

Vascular Adhesion Protein-1 siRNA Decreases VAP-1 Levels After Intracerebroventricular Injection

To examine the specificity of the antiinflammatory effects of VAP-1 inhibitors, VAP-1 siRNA as well as scramble siRNA (nontargeting siRNA) was given 48 hours before cICH induction. Protein levels of VAP-1 were then detected in the ipsilateral hemisphere by Western blot at 24 hours. In sham mice, siRNA injection significantly reduced VAP-1 levels ($P<0.05$, Figure 5A). Compared with scramble siRNA injection, VAP-1 levels in cICH mice were significantly decreased with siRNA injection

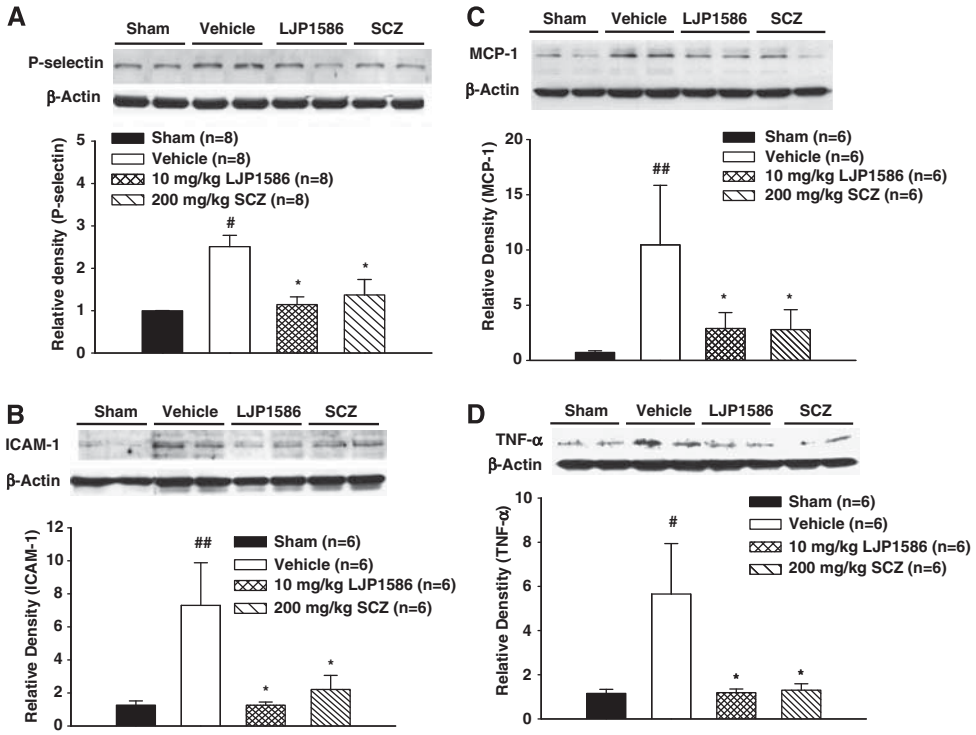

Figure 3 Adhesion molecules and proinflammatory cytokine levels were increased in vehicle group and decreased by vascular adhesion protein-1 (VAP-1) inhibitors 24 hours after collagenase-intracerebral hemorrhage (cICH) in mice. (**A**) Analysis of P-selectin level in ipsilateral hemisphere at 24 hours after ICH by Western blot. NS, nonsignificant. (**B**) Analysis of intercellular adhesion molecule-1 (ICAM-1) level in ipsilateral hemisphere at 24 hours after ICH by Western blot. (**C**) Analysis of monocyte chemoattractant protein-1 (MCP-1) level in ipsilateral hemisphere at 24 hours after ICH by Western blot. (**D**) Analysis of tumor necrosis factor-α (TNF-α) level in ipsilateral hemisphere at 24 hours after ICH by Western blot. All the brain samples were ipsilateral hemisphere collected from sham, ICH, and ICH with treatments (LJP1586: 10 mg/kg; semicarbazide (SCZ): 200 mg/kg). $^{\#\#}P < 0.01$ versus sham group. $^{\#}P < 0.05$ versus sham group. $^{*}P < 0.05$ versus vehicle group, $n = 6$ to 8.

($P < 0.05$, Figure 5A). In addition, neurobehavioral functions and brain edema were evaluated 24 hours post-cICH induction. Compared with cICH mice, the siRNA injected mice showed an improvement in neurobehavioral functions ($P < 0.05$ versus vehicle, Figure 5B). Moreover, brain edema in the ipsilateral basal ganglia was also significantly reduced (ipsilateral basal ganglia: siRNA + ICH, 81.73 ± 0.23 versus ICH, 82.75 ± 0.27, $P < 0.05$, Figure 5C).

Human Recombinant AOC3 (Vascular Adhesion Protein-1) Protein Abolishes the Antiinflammatory Effects of the Vascular Adhesion Protein-1 Inhibitor

The human recombinant AOC3 (VAP-1) protein was given as a neutralizer for LJP1586. The recombinant protein (30 ng/mouse, 90 ng/mouse) was given by intracerebroventricular injection 10 minutes before cICH induction. High-dose LJP1586 (10 mg/kg) was then administered 1 hour after cICH. Both neurobehavioral function and brain edema were evaluated 24 hours post-cICH.

In the modified Garcia test, both the low-dose (30 ng/mouse) and high-dose (90 ng/mouse) AOC3 protein markedly reversed the protective effects of LJP1586 treatment ($P < 0.05$, Figure 6A). For the wire-hanging and beam balance tests, high-dose AOC3 injected mice demonstrated a more severe neurobehavioral deficit than the ICH group alone. Compared with LJP1586-treated mice, neither low-dose nor high-dose AOC3 protein attenuated the effects of LJP1586 ($P < 0.05$ versus ICH + LJP, data not shown).

With regards to brain edema, the data showed that in the ipsilateral basal ganglia, high-dose AOC3 protein in cICH mice resulted in a markedly higher accumulation of edema than cICH mice alone (ipsilateral basal ganglia: 90 ng/mouse + ICH, 84.07 ± 0.39 versus ICH, 82.32 ± 0.30, $P < 0.05$, Figure 6B).

Both low-dose and high-dose AOC3 reversed the edema lowering effects of LJP1586 (ipsilateral basal ganglia: 30 ng/mouse + ICH + LJP1586, 82.57 ± 0.29 versus ICH + LJP1586, 80.94 ± 0.32, $P < 0.01$; 90 ng/mouse + ICH + LJP1586, 82.81 ± 0.30 versus ICH + LJP1586, 80.94 ± 0.32, $P < 0.01$, Figure 6B). In the ipsilateral cortex, there was no statistical significance found between the cICH mice group and the cICH plus AOC3 protein group. And finally, high-dose AOC3 protein (90 ng/mouse) significantly

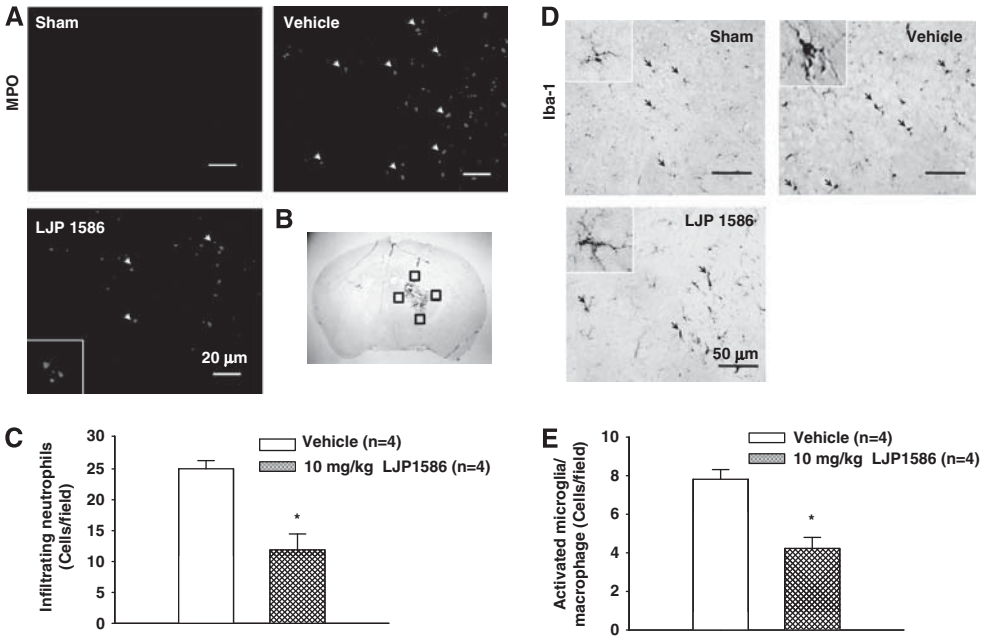

Figure 4 Effect of vascular adhesion protein-1 (VAP-1) inhibitor, LJP1586 on neutrophils infiltration and microglia/macrophage activation in the perihematomal region 24 hours after collagenase-intracerebral hemorrhage (cICH) in mice. (**A**) Represented photograph of immunofluorescence staining for myeloperoxidase (MPO) showing that the MPO-positive cells were increased in vehicle group and decreased in LJP1586 treatment (10 mg/kg) group at 24 hours after ICH. Sections from mice brain were probed with anti-MPO antibody and rabbit TX red secondary antibody (red). Scale bars, 20 μm. (**B**) The schematic diagram shows the four areas (black squares) for the MPO-positive cells counting in the perihematomal region. (**C**) Bar graph illustrating the quantification of MPO-positive cells in the perihematomal region at 24 hours in sham, vehicle, and LJP1586 treatment (10 mg/kg) (12 fields/brain). It showed that inhibition of VAP-1 significantly reduced the number of MPO-positive cells. (**D**) Represented photograph of immunohistochemistry staining for Iba-1-positive cells showed that the activated microglia/macrophage was increased in vehicle group and decreased in LJP1586 treatment (10 mg/kg) group 24 hours after ICH. Sections from mice brain were probed with rabbit anti-Iba1 antibody and goat anti-rabbit secondary antibody. Scale bars, 50 μm. (**E**) Bar graph illustrating the quantification of Iba-1-positive cells in vehicle and LJP1586 treatment (10 mg/kg) in the perihematomal region (12 fields/brain). The data revealed that VAP-1 inhibition by LJP1586 significantly reduced the number of activated Iba-1-positive cells. $^*P < 0.05$ versus vehicle group, $n = 4$. The color reproduction of this figure is available on the html full text version of the manuscript.

increased brain edema compared with the mice treated with LJP1586 (ipsilateral cortex: 90 ng/mouse + ICH + LJP1586, 80.672 ± 0.21 versus ICH + LJP1586, 79.58 ± 0.20, $P < 0.05$, Figure 6B).

Recombinant AOC3 Protein Reversed the Effect of Vascular Adhesion Protein-1 Inhibition on Migration of Systemic Neutrophils and Activation of Microglia/Macrophage

To further confirm the role of VAP-1 in inflammation, we evaluated the neutrophilic infiltration by MPO staining and microglia/macrophage activation by Iba-1 staining following recombinant AOC3 protein injection with LJP1586. In addition, quantification of both the MPO and Iba-1-positive cells in the perihematomal area were determined. Our results showed that there was no statistically significant difference in MPO-positive cell numbers between recombinant AOC3 protein administration with LJP1586 posttreatment mice and vehicle mice (24.48 ± 3.2, $n = 4$ and 25.27 ± 1.92, $n = 4$, respectively; $t_6 = 0.424$, $P = 0.69$; Figures 6C and 6D); whereas the microglia/macrophage activation failed to show a difference in the perihematomal area compared with vehicle mice (5.98 ± 0.83, $n = 4$ and 7.06 ± 0.86, $n = 4$, respectively; $t_6 = 0.905$, $P = 0.40$; Figures 6E and 6F).

Vascular Adhesion Protein-1 Inhibitors Improved Neurobehavioral Functions and Reduced Brain Edema in an Autologous Blood Injection Intracerebral Hemorrhage Model

Our results have suggested thus far that VAP-1 inhibition can significantly reduce brain edema and improve neurobehavioral functions in a cICH model. To strengthen these results, the autologous blood injection ICH model (bICH) was also applied to confirm the antiinflammatory effects of VAP-1 inhibition. Both VAP-1 inhibitors, LJP1586 and SCZ, were administered 1 hour after bICH induction in high concentrations (LJP1586, 10 mg/kg; SCZ, 200 mg/kg). Both neurobehavioral functions and

brain edema were evaluated at 24 hours. The results showed that treated mice performed markedly better in the modified Garcia test compared with vehicle mice ($P<0.05$, Figure 7A). In addition, compared with vehicle mice, both treatment groups had significantly reduced brain edema accumulations in the ipsilateral basal ganglia (ipsilateral basal ganglia: 10 mg/kg LJP1586, 80.59 ± 0.28 versus vehicle, 81.49 ± 0.15, $P<0.05$; 200 mg/kg SCZ, 80.58 ± 0.10 versus vehicle, 81.49 ± 0.15, $P<0.05$, Figure 7B).

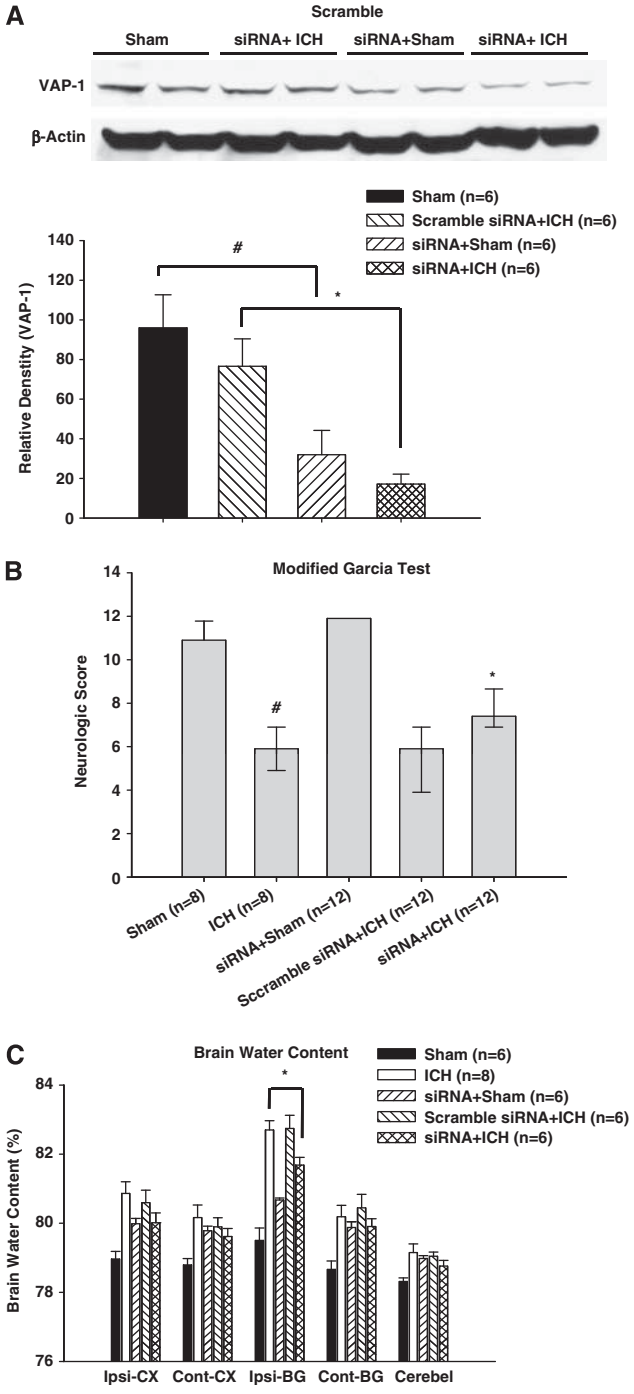

Discussion

Intracerebral hemorrhage is a fatal stroke subtype that currently has no effective treatment option. In this study, we investigated the effects of VAP-1 inhibition on ICH-induced brain injury. Specifically investigating the potential of this inhibition to reduce the migration of systemic immune cells to the site of injury and prevent the propagation of further parenchymal damage.

The ICH is induced in mice by either one of the two paradigms: by injection of autologous tail blood into the basal ganglia, or by injection of a clostridial bacterial collagenase into the basal ganglia (James *et al*, 2008). In the cICH model, formation of the hematoma is generated by direct disruption of blood vessels, mimicking a spontaneous ICH in humans (MacLellan *et al*, 2008). However, bacterial collagenase has been known to induce an exaggerated inflammatory response in the brain; although *in vitro* studies have refuted this hypothesis (Matsushita *et al*, 2000). As a result, to avoid the possible interference of bacterial collagenase in the normal inflammatory response after ICH, the autologous blood injection model was also used to verify the antiinflammatory properties of VAP-1 inhibition.

Vascular adhesion protein-1 is a homodimeric protein molecule present in a wide variety of cell types, including endothelial cells. Specifically, VAP-1 supports leukocyte adhesion by binding to and oxidatively deaminating a primary amino group presented on the leukocyte surface, resulting in the formation of a temporary bond between the two cell types (Salmi *et al*, 2001). Thus, blocking of VAP-1 would be expected to inhibit leukocyte migration.

Figure 5 Effect of vascular adhesion protein (VAP-1) siRNA on neurologic score and brain water content at 24 hours after collagenase-intracerebral hemorrhage (cICH) in mice. The VAP-1 siRNA was injected 48 hours before ICH and brain samples were collected 24 hours after ICH from sham, siRNA + sham, scramble siRNA + ICH, and siRNA + ICH. The VAP-1 siRNA was injected 48 hours before ICH, whereas neurobehavioral function and brain water content were evaluated 24 hours after ICH. The VAP-1 siRNA improved neurobehavioral functions and decreased brain water content 24 hours after collagenase-induced ICH in mice. (**A**) Western blotting with rabbit anti-VAP-1 antibody showed that the VAP-1 level in the ipsilateral hemisphere was reduced 72 hours after VAP-1 siRNA injection in a collagenase-induced intracerebral hemorrhage. (**B**) The neurologic score for the modified Garcia test (healthy animal: 12) at 24 hours in sham, siRNA + sham, ICH, non + ICH, and siRNA + ICH. (**C**) VAP-1 siRNA reduced brain water content 24 hours after ICH. Brain samples were collected from sham, siRNA + sham, ICH, nontargeting siRNA + sham, and siRNA + ICH. Brain sections (4 mm) were divided into four parts: ipsilateral basal ganglia (Ipsi-BG), ipsilateral cortex (Ipsi-CX), contralateral basal ganglia (Cont-BG), and contralateral cortex (Cont-CX). Cerebellum (Cerebel) is the internal control. 'non + ICH' presented nontargeting (scramble) siRNA + ICH. $^{\#}P<0.05$ versus sham group. $^{*}P<0.05$ versus vehicle group. For Western blot, $^{*}P<0.05$ versus Scramble siRNA + ICH group.

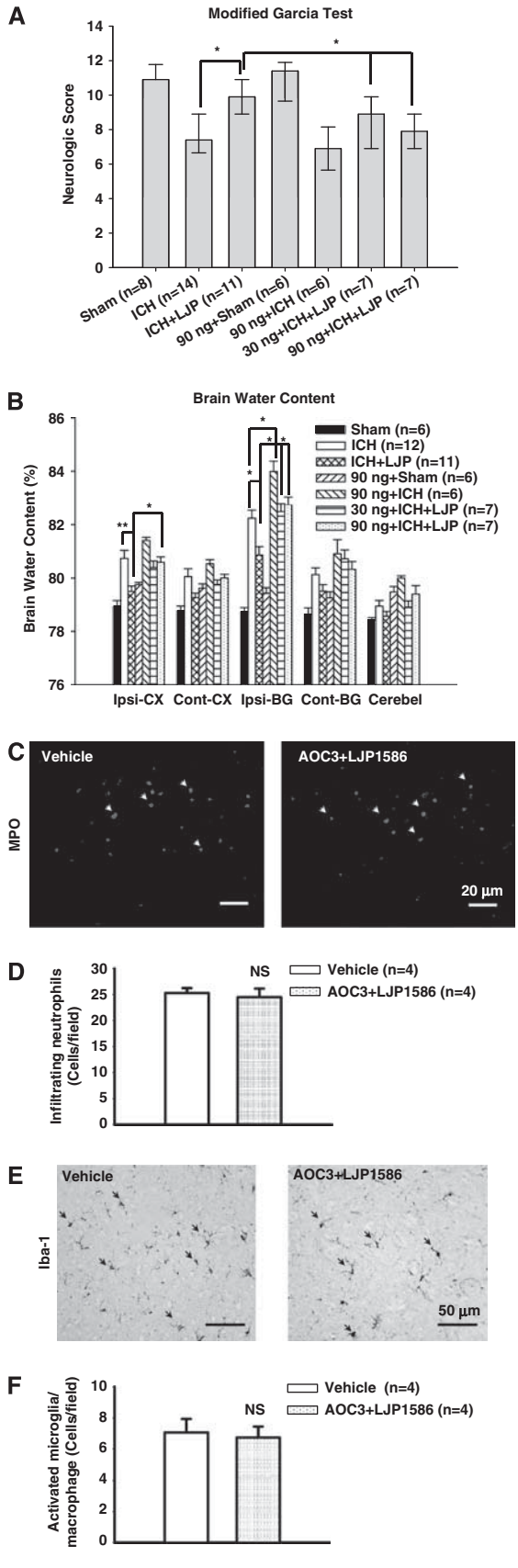

In our study, we found that VAP-1 inhibition down-regulated the adhesion molecule ICAM-1 and reduced the infiltration of systemic immune cells, specifically neutrophils, to the site of injury. In addition, with the reduction in systemic immune cells accumulating at the injury site, there was a marked reduction in proinflammatory cytokines, TNF-α and MCP-1, and a reduction in activation of microglial/macrophages. This prevented further propagation of the local immune response. Clinically, this translates into a significant reduction in cerebral edema accumulation and marked improvement in neurobehavioral function, which was the case at both 24 and 72 hours post-ICH.

Vascular adhesion protein-1's involvement in leukocyte infiltration has been studied in various experimental models. Most have implicated this protein as the key player in adhesion and transmigration of circulating systemic immune cells to the site of local injury. In ischemic models, VAP-1 has

Figure 6 Effect of recombinant AOC3 (vascular adhesion protein (VAP-1)) protein on neurologic score, brain water content, and neutrophils infiltration and microglia/macrophage activation at 24 hours after collagenase-intracerebral hemorrhage (cICH) in mice. Recombinant AOC3 protein was injected 10 minutes before ICH induction. (**A**) The neurologic score for the modified Garcia test (healthy animal: 12) at 24 hours after ICH in sham, ICH, ICH + LJP1586 (10 mg/kg), ICH + LJP1586 (10 mg/kg) + VAP-1 protein (30 ng/animal, 90 ng/animal), sham + VAP-1 protein (90 ng/animal), and ICH + VAP-1 protein (90 ng/animal). (**B**) Recombinant AOC3 protein reduced brain water content at 24 hours after ICH. Brain samples were collected from sham, ICH, ICH + LJP1586 (10 mg/kg), ICH + LJP1586 (10 mg/kg) + VAP-1 protein (30 ng/animal, 90 ng/animal), sham + VAP-1 protein (90 ng/animal), and ICH + VAP-1 protein (90 ng/animal). Brain sections (4 mm) were divided into four parts: ipsilateral basal ganglia (Ipsi-BG), ipsilateral cortex (Ipsi-CX), contralateral basal ganglia (Cont-BG), and contralateral cortex (Cont-CX). Cerebellum (Cerebel) is the internal control. (**C**) Represented photograph of immunofluorescence staining for myeloperoxidase (MPO) MPO-positive cell in vehicle group and recombinant AOC3 + LJP1586 treatment (10 mg/kg) group at 24 hours after ICH. Sections from mice brain were probed with anti-MPO antibody and rabbit TX Red secondary antibody (red). Scale bars, 20 μm. (**D**) Bar graph illustrating the quantification of MPO-positive cells in the perihematomal region at 24 hours in vehicle and recombinant AOC3 + LJP1586 treatment (10 mg/kg) (12 fields/brain). It showed that recombinant AOC3 abolished the effect of LJP1586 on reducing the number of MPO-positive cells. (**E**) Represented photograph of immunohistochemistry staining for Iba-1-positive cells in vehicle group and recombinant AOC3 + LJP1586 treatment (10 mg/kg) group 24 hours after ICH. Sections from mice brain were probed with rabbit anti-Iba1 antibody and goat anti-rabbit secondary antibody. Scale bars, 50 μm. (**F**) Bar graph illustrating the quantification of Iba-1-positive cells in vehicle and recombinant AOC3 + LJP1586 treatment (10 mg/kg) group in the perihematomal region (12 fields/brain). The data revealed that recombinant AOC3 abolish the effect of LJP1586 on reducing the number of activated Iba-1-positive cells. $^{**}P < 0.01$, $^{*}P < 0.05$; NS, nonsignificant. The color reproduction of this figure is available on the html full text version of the manuscript.

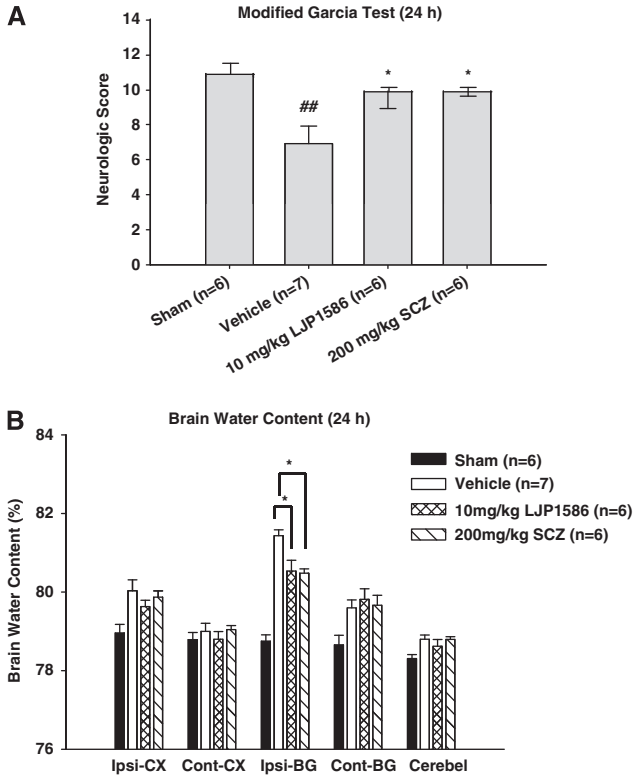

Figure 7 Vascular adhesion protein-1 (VAP-1) inhibitors, LJP1586 and semicarbazide (SCZ) improved neurologic score and decreased brain water content 24 hours after blood-intracerebral hemorrhage (bICH) in mice. (**A**) The neurologic score for the modified Garcia test (healthy animal: 12) at 24 hours in sham, ICH, and ICH with treatments (LJP1586: 10 mg/kg; SCZ: 200 mg/kg). (**B**) VAP-1 inhibitors, LJP1586 and SCZ reduced brain water content at 24 hours after autologous blood induced ICH in mice. Brain samples were collected from sham, ICH, and ICH with treatments (LJP1586: 10 mg/kg; SCZ: 200 mg/kg). Brain sections (4 mm) were divided into four parts: ipsilateral basal ganglia (Ipsi-BG), ipsilateral cortex (Ipsi-CX), contralateral basal ganglia (Cont-BG), and contralateral cortex (Cont-CX). Cerebellum (Cerebel) is the internal control. $^{\#\#}P < 0.01$ versus sham group. $^{*}P < 0.05$ versus vehicle group.

been shown to mediate leukocyte adhesion/infiltration in diabetic OVX females given chronic estrogen-replacement therapy (Xu *et al*, 2006). Studies on VAP-1 knockout mice found that the absence of VAP-1 led to abnormal leukocyte trafficking and attenuation of the inflammatory response in peritoneal infection (Stolen *et al*, 2005). In addition, *in vitro* studies have directly implicated VAP-1 in inducing E/P-selectin and ICAM-1 expression during inflammatory conditions in endothelial cells (Jalkanen *et al*, 2007). Studies investigating the relationship between VAP-1 and ocular inflammation found VAP-1 to be involved in leukocyte extravasations (Noda *et al*, 2008). Specifically, noting that VAP-1 inhibition reduced the expression of ICAM-1 and macrophage recruitment, while decreasing the secretion of proinflammatory markers TNF-α and MCP-1 to the choroidal tissue. In our study, we were able to show using immunohistochemistry that there was a strong presence of infiltrated neutrophils and activated microglia/macrophages around the hematoma region 24 hours after the cICH injury. In addition, treatment with the VAP-1 blocker LJP1586 significantly decreased the MPO-positive cell numbers and activated microglia/macrophages numbers, implying that VAP-1 mediates the infiltration of these systemic immune cells and propagation.

To strengthen our hypothesis that VAP-1 inhibition could provide antiinflammatory effects in ICH, we injected VAP-1 siRNA to knockdown VAP-1 expression. Our data showed that VAP-1 protein level in sham and cICH-operated mice were significantly reduced after VAP-1 siRNA injection, and also cICH-operated mice showed a lower VAP-1 level than sham. The same phenomenon has been reported in human ischemic stroke models (Airas *et al*, 2008). The study by Airas *et al* showed that in the acute phase of ischemic stroke, VAP-1-positive vessels were strongly diminished in the ipsilateral hemisphere, but the VAP-1 levels in the serum were significantly increased. In addition, we introduced human recombinant AOC3 protein to neutralize the effects of LJP1586. Our data showed that both low-dose and high-dose exogenous VAP-1 protein delivery counteracted the effect of VAP-1 inhibitor. It produced a worse performance in cICH mice with VAP-1 inhibition, and restored brain edema back to the level of the cICH mice. We also found that the administration of exogenous VAP-1 protein exacerbated neurobehavioral deficits and brain edema in cICH mice and only slightly worsened it in sham mice.

One limitation of our study is the injection pattern of siRNA and human recombinant VAP-1 protein. Although we have no direct evidence that siRNA and recombinant protein may cross the blood–brain barrier, previous studies have shown that following cICH, there is a marked increase in blood–brain barrier permeability by 30 minutes, which is maintained from 5 hours to 7 days, with normal permeability being restored by day 14 (Rosenberg *et al*, 1993).

In conclusion, this study shows that VAP-1 inhibition ameliorates ICH-induced brain damage in adult male mice by attenuating the adhesion and transmigration of circulating systemic immune cells to the site of local injury. By doing so, VAP-1 inhibition prevents the propagation of the local inflammatory process and in turn, reduces cerebral edema, improves neurobehavioral function, and may act as a potential therapeutic target for future clinical direction.

Acknowledgements

The authors thank La Jolla Pharmaceutical Company, San Diego, CA, provided VAP-1 inhibitor, LJP1586.

Disclosure/conflict of interest

The authors declare no conflict of interest.

References

Airas L, Lindsberg PJ, Karjalainen-Lindsberg ML, Mononen I, Kotisaari K, Smith DJ, Jalkanen S (2008) Vascular adhesion protein-1 in human ischaemic stroke. *Neuropathol Appl Neurobiol* 34:394–402

Aronowski J, Hall CE (2005) New horizons for primary intracerebral hemorrhage treatment: experience from preclinical studies. *Neurol Res* 27:268–79

Barone FC, Feuerstein GZ (1999) Inflammatory mediators and stroke: new opportunities for novel therapeutics. *J Cereb Blood Flow Metab* 19:819–34

Belayev L, Saul I, Curbelo K, Busto R, Belayev A, Zhang Y, Riyamongkol P, Zhao W, Ginsberg MD (2003) Experimental intracerebral hemorrhage in the mouse: histological, behavioral, and hemodynamic characterization of a double-injection model. *Stroke* 34:2221–7

Chen W, Jadhav V, Tang J, Zhang JH (2008) HIF-1alpha inhibition ameliorates neonatal brain injury in a rat pup hypoxic-ischemic model. *Neurobiol Dis* 31:433–41

Dennis MS, Burn JP, Sandercock PA, Bamford JM, Wade DT, Warlow CP (1993) Long-term survival after first-ever stroke: the Oxfordshire Community Stroke Project. *Stroke* 24:796–800

Emsley HC, Tyrrell PJ (2002) Inflammation and infection in clinical stroke. *J Cereb Blood Flow Metab* 22:1399–419

Garcia JH, Wagner S, Liu KF, Hu XJ (1995) Neurological deficit and extent of neuronal necrosis attributable to middle cerebral artery occlusion in rats. Statistical validation. *Stroke* 26:627–34; discussion 635

Gerlai R, Thibodeaux H, Palmer JT, van Lookeren Campagne M, Van Bruggen N (2000) Transient focal cerebral ischemia induces sensorimotor deficits in mice. *Behav Brain Res* 108:63–71

Jalkanen S, Karikoski M, Mercier N, Koskinen K, Henttinen T, Elima K, Salmivirta K, Salmi M (2007) The oxidase activity of vascular adhesion protein-1 (VAP-1) induces endothelial E- and P-selectins and leukocyte binding. *Blood* 110:1864–70

James ML, Warner DS, Laskowitz DT (2008) Preclinical models of intracerebral hemorrhage: a translational perspective. *Neurocrit Care* 9:139–52

Koskinen K, Vainio PJ, Smith DJ, Pihlavisto M, Yla-Herttuala S, Jalkanen S, Salmi M (2004) Granulocyte transmigration through the endothelium is regulated by the oxidase activity of vascular adhesion protein-1 (VAP-1). *Blood* 103:3388–95

Luo J, Wang Y, Chen X, Chen H, Kintner DB, Shull GE, Philipson KD, Sun D (2007) Increased tolerance to ischemic neuronal damage by knockdown of Na^+-$Ca2^+$ exchanger isoform 1. *Ann N Y Acad Sci* 1099:292–305

MacLellan CL, Silasi G, Poon CC, Edmundson CL, Buist R, Peeling J, Colbourne F (2008) Intracerebral hemorrhage models in rat: comparing collagenase to blood infusion. *J Cereb Blood Flow Metab* 28:516–25

Matsushita K, Meng W, Wang X, Asahi M, Asahi K, Moskowitz MA, Lo EH (2000) Evidence for apoptosis after intercerebral hemorrhage in rat striatum. *J Cereb Blood Flow Metab* 20:396–404

Mercier N, El Hadri K, Osborne-Pellegrin M, Nehme J, Perret C, Labat C, Regnault V, Lamaziere JM, Challande P, Lacolley P, Feve B (2007) Modifications of arterial phenotype in response to amine oxidase inhibition by semicarbazide. *Hypertension* 50:234–41

Noda K, She H, Nakazawa T, Hisatomi T, Nakao S, Almulki L, Zandi S, Miyahara S, Ito Y, Thomas KL, Garland RC, Miller JW, Gragoudas ES, Mashima Y, Hafezi-Moghadam A (2008) Vascular adhesion protein-1 blockade suppresses choroidal neovascularization. *FASEB J* 22: 2928–35

O'Rourke AM, Wang EY, Miller A, Podar EM, Scheyhing K, Huang L, Kessler C, Gao H, Ton-Nu HT, Macdonald MT, Jones DS, Linnik MD (2008) Anti-inflammatory effects of LJP 1586 [Z-3-fluoro-2-(4-methoxybenzyl)allylamine hydrochloride], an amine-based inhibitor of semicarbazide-sensitive amine oxidase activity. *J Pharmacol Exp Ther* 324:867–75

Ostrowski RP, Colohan AR, Zhang JH (2005) Mechanisms of hyperbaric oxygen-induced neuroprotection in a rat model of subarachnoid hemorrhage. *J Cereb Blood Flow Metab* 25:554–71

Ribo M, Grotta JC (2006) Latest advances in intracerebral hemorrhage. *Curr Neurol Neurosci Rep* 6:17–22

Rosenberg GA, Estrada E, Kelley RO, Kornfeld M (1993) Bacterial collagenase disrupts extracellular matrix and opens blood-brain barrier in rat. *Neurosci Lett* 160:117–9

Rosenberg GA, Mun-Bryce S, Wesley M, Kornfeld M (1990) Collagenase-induced intracerebral hemorrhage in rats. *Stroke* 21:801–7

Rynkowski MA, Kim GH, Komotar RJ, Otten ML, Ducruet AF, Zacharia BE, Kellner CP, Hahn DK, Merkow MB, Garrett MC, Starke RM, Cho BM, Sosunov SA, Connolly ES (2008) A mouse model of intracerebral hemorrhage using autologous blood infusion. *Nat Protoc* 3:122–8

Salmi M, Jalkanen S (1992) A 90-kilodalton endothelial cell molecule mediating lymphocyte binding in humans. *Science* 257:1407–9

Salmi M, Jalkanen S (2005) Cell-surface enzymes in control of leukocyte trafficking. *Nat Rev Immunol* 5:760–71

Salmi M, Yegutkin GG, Lehvonen R, Koskinen K, Salminen T, Jalkanen S (2001) A cell surface amine oxidase directly controls lymphocyte migration. *Immunity* 14: 265–76

Stolen CM, Marttila-Ichihara F, Koskinen K, Yegutkin GG, Turja R, Bono P, Skurnik M, Hanninen A, Jalkanen S, Salmi M (2005) Absence of the endothelial oxidase AOC3 leads to abnormal leukocyte traffic *in vivo*. *Immunity* 22:105–15

Tang J, Liu J, Zhou C, Alexander JS, Nanda A, Granger DN, Zhang JH (2004) Mmp-9 deficiency enhances collagenase-induced intracerebral hemorrhage and brain injury in mutant mice. *J Cereb Blood Flow Metab* 24: 1133–45

Tang J, Liu J, Zhou C, Ostanin D, Grisham MB, Neil Granger D, Zhang JH (2005) Role of NADPH oxidase in the brain injury of intracerebral hemorrhage. *J Neurochem* 94: 1342–50

Tejima E, Zhao BQ, Tsuji K, Rosell A, van Leyen K, Gonzalez RG, Montaner J, Wang X, Lo EH (2007) Astrocytic induction of matrix metalloproteinase-9 and edema in brain hemorrhage. *J Cereb Blood Flow Metab* 27:460–8

Titova E, Ostrowski RP, Kevil CG, Tong W, Rojas H, Sowers LC, Zhang JH, Tang J (2008) Reduced brain injury in CD18-deficient mice after experimental intracerebral hemorrhage. *J Neurosci Res* 86:3240–5

Wang J, Dore S (2007) Inflammation after intracerebral hemorrhage. *J Cereb Blood Flow Metab* 27:894–908

Wang J, Dore S (2008) Heme oxygenase 2 deficiency increases brain swelling and inflammation after intracerebral hemorrhage. *Neuroscience* 155:1133–41

Wang J, Fields J, Dore S (2008) The development of an improved preclinical mouse model of intracerebral hemorrhage using double infusion of autologous whole blood. *Brain Res* 1222:214–21

Wu B, Ma Q, Khatibi N, Chen W, Sozen T, Cheng O, Tang J (2010) Ac-YVAD-CMK decreases blood–brain barrier degradation byInhibiting caspase-1 activation of interleukin-1β in intracerebral hemorrhage mouse model. *Transl Stroke Res (Accepted)* 1:57–64

Xu HL, Salter-Cid L, Linnik MD, Wang EY, Paisansathan C, Pelligrino DA (2006) Vascular adhesion protein-1 plays an important role in postischemic inflammation and neuropathology in diabetic, estrogen-treated ovariectomized female rats subjected to transient forebrain ischemia. *J Pharmacol Exp Ther* 317:19–29

Yilmaz G, Granger DN (2008) Cell adhesion molecules and ischemic stroke. *Neurol Res* 30:783–93

Zausinger S, Hungerhuber E, Baethmann A, Reulen H, Schmid-Elsaesser R (2000) Neurological impairment in rats after transient middle cerebral artery occlusion: a comparative study under various treatment paradigms. *Brain Res* 863:94–105